Journal of Ceramic Processing Research. Vol. 26, No. 1, pp. 9~22 (2025)
(Received 30 July 2024, Received in revised form 3 February 2025, Accepted 5 February 2025)
https://doi.org/10.36410/jcpr.2025.26.1.9

J O U R N A L O F
Ceramic Processing Research

Evolutionary reactions for hydrogen production efficiency improved in various ways by TiO_2 modification: a review

Yu Sun and ZhiRu. Zhao*
Yingkou Institute of Technology, Liaoning, China

In the context of rapid urbanisation and industrialisation, traditional fossil energy fuels have been over-consumed, which has led to increasingly serious energy problems and a series of environmental issues. Hydrogen energy, which is known to us as a clean energy, is the most ideal alternative to traditional energy sources. Solar photocatalytic and photoelectrochemical water splitting to produce hydrogen is an energy conversion process that converts solar energy into chemical energy. As a new hydrogen production technology, it is undoubtedly one of the best means to solve energy and environmental problems. As one of the most researched photocatalytic materials, TiO_2 has a series of advantages such as not easy to be photocorroded or chemically corroded during the reaction, pollution-free, cheap and easy to obtain. But it also has certain disadvantages, such as a large forbidden bandwidth coefficient, the influence of its own crystalline phase, and the low utilisation of visible light, etc. In order to better solve the defects of TiO_2, this paper focuses on exploring the development of photocatalytic hydrogen-producing materials with low cost and high efficiency of hydrogen production. It reviews the photocatalytic and photoelectrochemical mechanism of TiO_2, which analyses the influence of TiO_2 itself on its own phase as well as other aspects of the limitations of the TiO_2 and also can be used to address the corresponding countermeasures for these problems. In this paper, the methods of doping metal ions, non-metal ion doping and heterojunction construction of TiO_2 semiconductor catalyst water splitting were raised in order to enhance the performance of hydrogen evolution. Doping metal and non-metal ions can inhibit the complexation of electrons and holes as a way to increase the forbidden bandwidth. Moreover, the contracting heterojunction is an effective solution to boost the performance of TiO_2 hydrogen evolution. As one of the most commonly used and optimal photocatalytic materials, TiO_2 is of great significance to explore and improve its photocatalytic efficiency. The above methods can be used to improve the photocatalytic efficiency of TiO_2. The above-mentioned methods can improve the photocatalytic efficiency of photocatalytic materials, which can help to break through a major problem in today's research, and lay a solid foundation for the rapid development of TiO_2 photocatalytic reaction technology for hydrogen production.

Keywords: TiO_2, Hydrogen evolution, Ion doping, Heterojunction construction, Water splitting.

Introduction

Nowadays, the most significant of environmental problems is the greenhouse effect caused by CO_2 discharge, which brings many potential impacts on the global climate [1-3]. The dangerous of global climate changes bring us including that the melting of glaciers triggered by the rise in sea level, threatening the inhabitants of coastal cities and islands [4]. Moreover, climate change may also lead to an increase in the number of droughts and floods in some areas, threatening agricultural production, and uncertainty about food security and water supply [5]. It may also lead to increased droughts and floods in some areas, threats to agricultural production, and uncertainty about food security and water supplies [6]. Hence, a cleaner type of energy is urgently needed by mankind: hydrogen energy. Hydrogen energy, as an energy source with a wide range of applications, has excellent advantages. Hydrogen energy is a zero-emission clean energy source, the only exhaust gas produced by its combustion is water vapor, which has no harmful gases, and is therefore non-polluting to the environment [7].

Currently, the main method of hydrogen production is industrial by-production, which is a technology based on the principle of obtaining hydrogen from the by-products of industrial processes [8]. Conventional industrial by-production methods usually produce limited amounts of hydrogen, are energy-intensive, and generate large amounts of greenhouse gases. However, the production of hydrogen is not limited to this method, for example, hydrogen production by water gas method [9], bio-hydrogen [10] and hydrogen production by electrolysis of water [11]. In this case, hydrogen by water gas method involves passing water vapor through scorched coke to end up with hydrogen with a purity of about

*Corresponding author:
Tel : 15840720898
Fax: 3588500
E-mail: zhaozhiru@yku.edu.cn

75%. The advantages are that it is less expensive and can be used on a larger scale, but the hydrogen produced has a high sulfur content [10]. Bio-fermentation of hydrogen, a technology that uses biological or photobiological methods to produce hydrogen from renewable resources such as water, organic waste or biomass, is called biohydrogen production, and the corresponding hydrogen is called biohydrogen [11]. Bio-fermentation hydrogen production technology has the advantages of a wide range of raw materials, low production costs and non-pollution. However, it has the disadvantage of covering a large area and is not suitable for large-scale production [12]. Hydrogen production by electrolysis of water usually involves placing two electrodes into water in an electrolytic cell, where electricity is added to break down water molecules into ions, which in turn produces hydrogen and oxygen. It has ushered in a broad space for development due to its environmental friendliness, simple process and high purity of hydrogen production [13]. But its disadvantage is that it consumes too much electricity and costs too much [14].

Solar energy, the fastest-growing renewable energy source, provides a constant supply of light energy, which has led to a great deal of interest among scientists in the use of photochemistry to produce hydrogen. Since Fujishima and Honda adopted n-type TiO_2 to prepare hydrogen in 1972, photocatalyst and photoelectrochemical water splitting for hydrogen evolution are considered as an ideal way to generate hydrogen via using direct sun irradiation [15]. The principle of photocatalyst is that under the action of light, semiconductor photocatalysts generate photogenerated electron-hole pairs. For some semiconductor photocatalysts, the photogenerated electron-hole pairs generated have two functions of strong reduction and oxidation ability, thus semiconductor photocatalysts have a wide range of applications in the fields of purification of pollutants, photolysis of water to produce hydrogen, and the synthesis and conversion of substances [16-18]. The mechanism of photoelectrochemical is to add a bias voltage to photocatalysis, so that the photogenerated electrons on the surface of the catalyst can be transferred to the photocathode through a wire, and a reduction reaction occurs to produce hydrogen. On the surface of the catalyst photoanode, an oxidation reaction occurs to produce oxygen [19, 20]. Both have the advantages of being environmentally independent, highly efficient, environmentally friendly, favorable to recycling, and having a wide range of applications.

The most important of photocatalyst and photoelectrochemical is the material for catalyst, including the g-C_3N_4 [21], ZnO [22, 23], CdS [24] and TiO_2 [18, 25]. Wang et al. [26] prepared g-C_3N_4 stretcher-loaded Pt-Ag atom-pair photocatalysts for photocatalytic water splitting demonstrated outstanding hydrogen production performance, obtaining a high hydrogen precipitation rate of 3480 μmol g^{-1} h^{-1}. Feng et al. [27] reported a new CdS@ZnO core-shell nanorod arrays is successfully constructed by atomic layer deposition (ALD) for H_2 evolution from photoelectrochemical water splitting. The photoelectrochemical H_2 evolution rate raised 21.64 μmol·h^{-1}·cm^{-2}. Among the numerous catalysts, TiO_2 was intensively studied as a typical material. TiO_2 has multiple advantages: its stability, chemical stability and thermal stability is high, in the reaction is not easy to photocorrosion or chemical corrosion, and TiO_2 photocatalytic activity is high, no pollution, friendly to the environment, cheap and easy to get [28]. However, TiO_2 is still insufficient in some aspects, for example, the most important disadvantage of TiO_2 photocatalyst is that the photogenerated carriers are extremely easy to compound, because of its own low conductivity, which restricts the separation of the photogenerated carriers, and the electrons return to the valence band and compound with the holes after they are excited by the light, which decreases the utilization rate of carriers, and thus leads to the decrease in the efficiency of the photo-quantum [29]. Moreover, the band gap of TiO_2 is wide, with a forbidden band width of 3.2 eV, which can only respond to ultraviolet light at wavelengths of 387 nm, seriously affecting the response range of visible light, lowering the utilization rate of visible light, and restricting its industrialized application [30].

For dealing with the shortcoming of TiO_2 in photocatalyst and photoelectrochemical water splitting for H_2 evolution, doping foreign ions [31], constructing heterojunctions [32] and addition of co-catalyst [33] are common methods to enhance the performance of TiO_2 catalyst. Chen et al. [34] prepared Ce-La-Ag co-doped TiO_2/basalt fiber composite photocatalysts by sol-gel method, and the band gap was reduced from 3.20 eV to 2.15 eV, the photocatalytic activity was significantly improved. Lin et al. [32] constructed WO_{3-x}/TiO_2 Z-scheme heterojunction for overall water splitting producing H_2. An optimum photoelectrochemical activity was achieved over a WO_{3-x}/TiO_2 photoelectrode yielding maximum H_2 and O_2 evolution rates roughly 11 times higher than that of pure TiO_2 nanorods without any sacrificial agent or redox mediator. Ali et al. [35] proposed the decoration of a Fe-Ni-based cocatalyst on the surface of the TiO_2 photoanode for photoelectrochemical water splitting. The TiO_2 photoanode was hydrothermally synthesized and then decorated by Fe-Ni hydroxide catalyst using photo-assisted electrodeposition. The TiO_2/FeNiOOH photoanode great photocatalytic activity compared to TiO_2. Although there have been many reports on TiO_2 modification to promote photocatalyst and photoelectrochemical decomposition of aqueous hydrogen, there is a lack of articles summarizing the relevant methods and mechanisms. Therefore, this thesis describes the advantages and disadvantages, as well as the limitations of the TiO_2 modification approach, and provides an outlook on the existing improvements and potential possibilities.

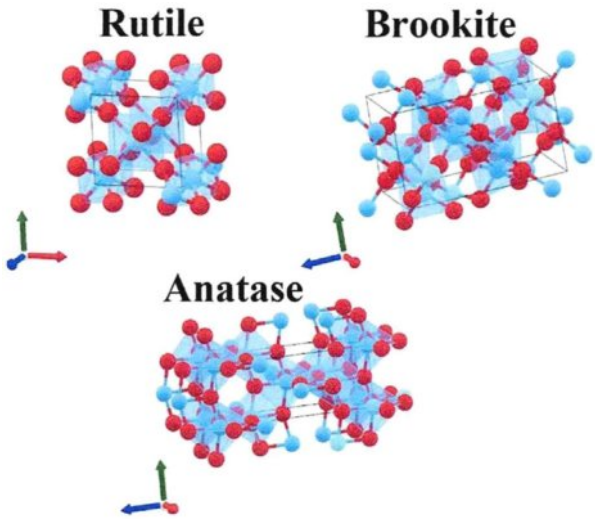

Fig. 1. Three crystal structures of TiO_2: rutile, anatase and brookite [36].

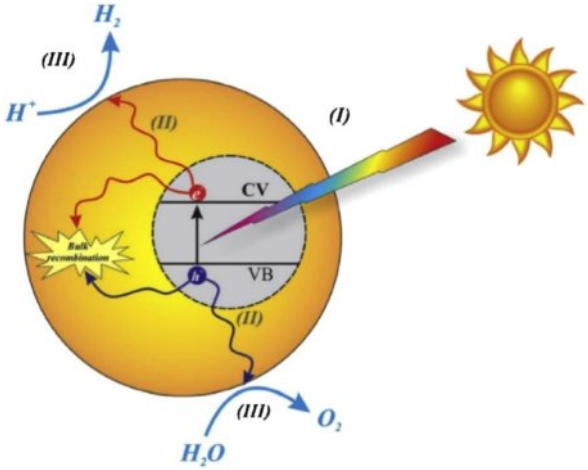

Fig. 2. Schematic representation of the important steps in photocatalytic water splitting using TiO_2 [44].

Crystalline Structure of TiO_2 and its Photocatalytic Mechanism

In nature, TiO_2 mainly exists in the following three crystal forms: rutile, brookite and anatase in Fig. 1 [36]. These three crystal forms also have their own characteristics. The first is rutile type, whose crystal is slender and prismatic, usually twin. The rutile TiO_2 is also the most stable crystalline form of TiO_2 as shown, with dense structure, high hardness, density, dielectric constant, refractive index and high adsorption capacity. As the most stable crystal form, rutile TiO_2 has more stable physical and chemical properties and excellent pigment performance [37]. The crystal form of brookite TiO_2 belongs to orthorhombic system. Six TiO_2 molecules form a cell, which belongs to unstable compound [38]. The basic unit of these three structures is a TiO_6 octahedron composed of one Ti atom and six zero atoms, but the connection forms of the TiO_6 octahedron are different. The Ti_6 octahedron of rutile structure TiO_2 forms a linear chain arrangement in the form of common edge and common vertex, the TiO_6 octahedron of anatase structure TiO_2 forms a zigzag chain arrangement in the form of common edge, and the TiO_6 octahedron of anatase structure TiO_2 is between rutile structure and anatase structure, cross arranged in the form of common edge and common vertex. For anatase type, its shape is generally similar to regular octahedron. Because its unit lattice is composed of two TiO_2 molecules, it has greater stability and relative density. Compared with rutile TiO_2, anatase has low hardness, density, dielectric constant and refractive index, and low thermal conductivity [39].

The photocatalyst mechanism of TiO_2 refers to that under light, the catalyst absorbs light energy and produces active intermediates to promote the reaction by contacting with reactants and transferring electrons or holes as shown in Fig. 2. The so-called photocatalyst technology is a new environmental protection technology that uses light energy to promote material reaction. As for photocatalysis, the most important thing is about catalysts. Because of its good light absorption performance, TiO_2 has become a commonly used catalyst [40, 41]. There are many active sites on the surface of the catalyst, which can adsorb reactants and produce active intermediates. In addition, there are electron and hole pairs on the surface of the catalyst. During the process of light excitation, the electrons and holes are continuously transferred on the surface of the catalyst, forming charge pairs. The two also have different roles in the photocatalytic reaction. Electrons usually participate in the oxidation reaction, while holes participate in the reduction reaction. According to the different modes of action of photons with catalysts and adsorbed materials, catalytic reactions can be divided into sensitized photoreaction and catalyzed photoreaction, whose essence is that the transfer direction of charge is different [42, 43]. The e^-/h^+ generated in the sensitized photoreaction flows from the catalyst to the adsorbed molecule, while the charge flow direction of the catalytic photoreaction is just opposite. For e^-/h^+, its migration rate and probability depend on the position of the lowest level conduction band and the highest level valence band, as well as the redox potential of the adsorbed material. The core of photocatalyst technology is photocatalysis mechanism, including catalyst, photoexcitation process, charge transfer process and many other aspects [44].

Photoelectrochemical is a catalytic method based on the combination of multiphase photocatalyst oxidation technology and electrochemistry, which refers to the formation of an internal electric field when the catalyst is irradiated by visible or ultraviolet light in Fig. 3 [45]. The interaction between the internal electric field and the external electric field elevates the electrons from the valence band of the semiconductor photocatalyst to the

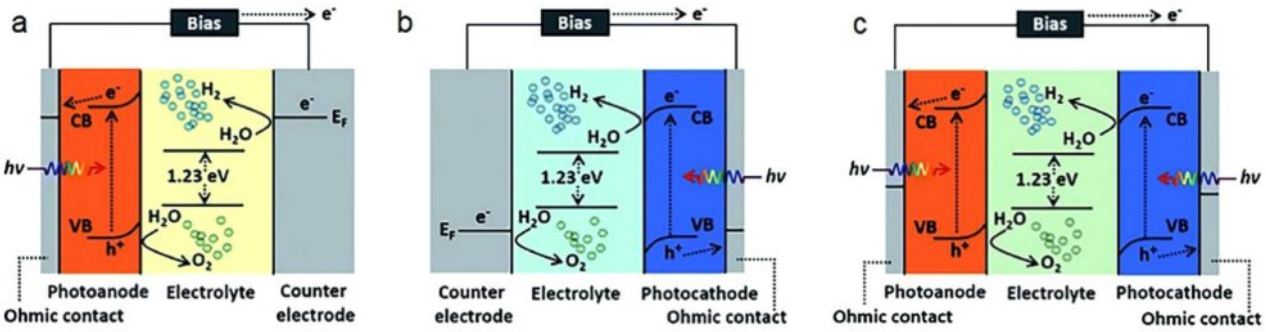

Fig. 3. PEC water splitting systems (a) a photoanode (b) a photocathode (c) photoanode and photocathode with their detailed mechanisms in the energy band [45].

conduction band. The bonded electrons in the catalyst will be activated, thus generating electron-hole pairs, which are widely recognized because of the strong oxidation-reduction ability. These electron-hole pairs have attracted much attention because of their strong redox ability. photoelectrochemical has many advantages, such as: its catalytic reaction is photochemical reaction, which does not produce chemical pollutants and does not require the use of chemical catalysts, and does not produce secondary pollution; the preparation technology of the required catalyst materials is mature, and can be easily prepared; photoelectrochemical reaction can be carried out at low temperature, low pressure and anhydrous conditions, and the efficiency is high. photoelectrochemical is also an effective way to convert solar energy into chemical energy, thus realizing large-scale solar energy utilization [46].

Techniques for Synthesizing TiO_2 Nanomaterials

The synthesis strategies of TiO_2 have been extensively studied as a traditional material. In this section, we will discuss three common and widely used synthesis strategies.

Hydrothermal synthesis

Hydrothermal synthesis is usually carried out in a concave furnace using an aqueous solution at a temperature that can be raised above the boiling point of water to reach saturation pressure under controlled pressure and temperature conditions. This method is widely used in the ceramic industry for the production of small particles [47-49]. Many research groups have utilized the hydrothermal method to synthesize TiO_2 nanoparticles. For instance, Lin et al. demonstrated the modulation of the TiO_2 phase composition by a hydrothermal method as shown in Fig. 4a [50]. Their method consisted of adding 1 ml of NH_3-H_2O and 62 ml of deionized water to 100 ml of a Teflon sealed autoclave at room temperature, followed by the rapid addition of 5 ml of $TiCl_3$ to the solution. The resulting suspension was centrifuged, and the collected solid product was washed three times thoroughly with ethanol and water, and then dried for 8 h at 80 °C. Chuangchote describe a straightforward method to create TiO_2 nanofibers using a combination of electrospinning and sol-gel techniques. This involves using polyvinylpyrrolidone, titanium butoxide, and acetylacetone in methanol as a spinning solution. After calcination of the TiO_2/PVP composite fibers at temperatures between 300 and 700 °C, we obtained TiO_2 nanofibers (260-355 nm in diameter) with either aligned nanofibrils (20-25 nm in diameter) or particle-linked structures. Its shape is shown in Fig. 4b [51]. The findings suggest that electrospun nanofibers with aligned bundled nanofibrils contribute to improved crystallinity, increased surface area, and enhanced photocatalytic activity. Li et al. utilized a microemulsion-mediated hydrothermal method to produce TiO_2 particles with adjustable morphology and heightened photoactivity. As the hydrothermal temperature rose, the particles exhibited an increase in average pore size, crystal size, and crystallinity, alongside a decrease in specific surface area. Moreover, there was a transition in morphology from spherical to rod-like structures. Figure 4c illustrates this transition, attributing it to a decrease in microemulsion interfacial strength and an increase in droplet collision efficiency with rising hydrothermal temperature [52]. This suggests a mechanism for the morphological transformation of TiO_2.

Hydrothermal and solvothermal techniques have been employed to fabricate various TiO_2-based photocatalysts, including TiO_2/graphene hybrids graphene [53, 54], oxide/TiO_2 (RGOT) aerogels [55] and TiO_2/metal-organic framework (MOF) composites [56]. In a study by Zhang et al. presents a sustainable method for synthesizing chemically bonded TiO_2/graphene sheets (GS) nanocomposites via a one-step hydrothermal process [53]. The photocatalytic hydrogen evolution was notably improved with the TiO_2/GS composite photocatalysts, showing a 1.6 times larger enhancement the pure TiO_2. This fabrication method involves the concurrent reduction of graphene oxide and formation of TiO_2, resulting in the well-dispersed TiO_2 nanoparticles

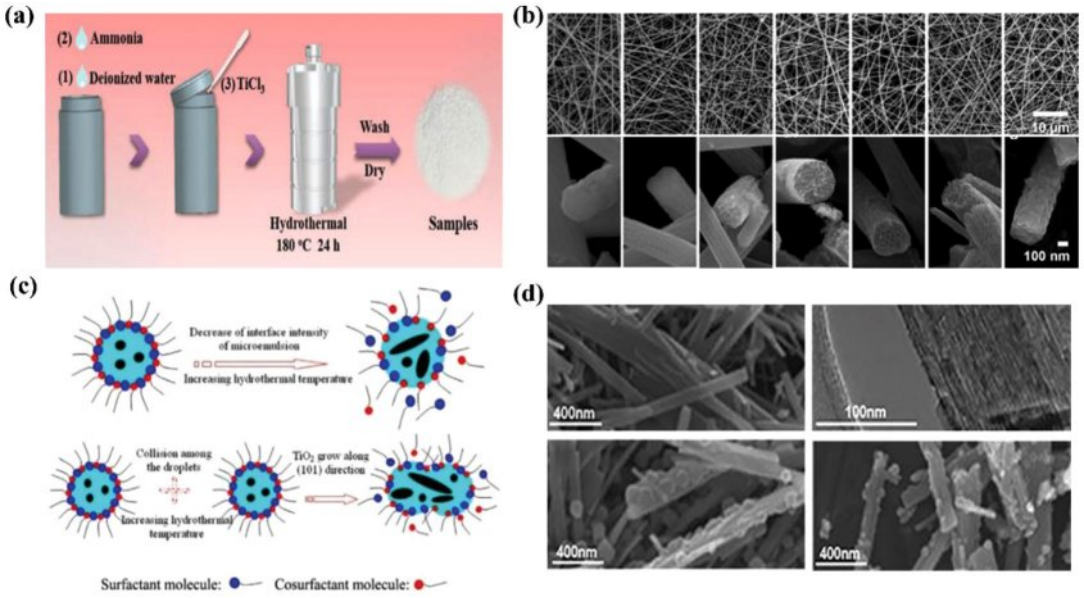

Fig. 4. Hydrothermal methods for synthesizing TiO_2 nanomaterials. (a) Schematic diagram of the process of preparing TiO_2 nanocrystals, (b) SEM images of PVP/TiO_2 composite nanofibers and TiO_2 nanofibers after calcination at various temperatures (c) morphology regulation mechanism of TiO_2 nanoparticles prepared by microemulsion-mediated hydrothermal method, (d) Electron microscope images of titanate fibers (t), t-300-MOF composites, anatase fibers (T) and T-300-MOF composites.

on the GS surface. Nawaz et al. developed three-dimensional reduced graphene oxide/titanium dioxide (RGOT) aerogels through a straightforward one-step heat treatment process, enabling the creation of well-defined structures with improved characteristics [53]. Field emission scanning electron microscopy (FE-SEM) images depicting reduced graphene oxide (RGO) and RGOT. Jiang et al. [57] also investigated TiO_2/graphene composites for wastewater treatment via hydrothermal synthesis. Their research revealed that the photocatalytic efficiency of the composite containing 18% TiO_2/graphene content was 5.43 times higher than that of pure TiO_2, indicating the performance enhancement achieved by incorporating graphene into TiO_2-based photocatalysts. Crake et al. focused on the preparation of TiO_2/metal-organic frame work (MOF) composites [56]. The synthesis process involved dissolving 5 g of titanium oxide particles (P25) in 70 ml of 10 mol/L NaOH, followed by hydrogen ether mal treatment. Subsequent steps included acid washing, water washing, and microwave antenna synthesis, resulting in the formation of TiO_2 nanofibers, t-MOF, and T-300-MOF composites. The structural characteristics of titanate, T, t-MOF, and T-300-MOF are illustrated in the electron microscope images presented in Fig. 4d.

Solvothermal synthesis

The basic principle of solvothermal and hydrothermal methods is the same, the only difference is that the solvent is changed from an aqueous solution to an organic solvent. Indeed, solvothermal synthesis has emerged as a prominent method for producing nanoparticles with precise control over size distribution and dispersion [58, 59]. The choice of solvent plays a crucial role in creating an optimal reaction environment to achieve desired material properties. Organic solvents commonly employed in solvothermal synthesis, such as N, N-dimethylformamide and N, N-dimethylacetamide exhibit both polar and non-volatile characteristics [60]. These solvents possess high solubility for various precursors, facilitating nanoparticle dissolution, nucleation, and subsequent growth. Utilizing solvents with elevated boiling points enables solvothermal reactions to be conducted at high temperatures and pressures within a sealed autoclave, ensuring efficient synthesis processes. These solvents, with their broad solubility for various precursors, facilitate the dissolution of nanoparticles and subsequent growth through nucleation. Solvothermal reactions, conducted under high temperatures and pressures within sealed autoclaves using high-boiling point solvents, create a controlled environment conducive to dissolution and diffusion of reactants, leading to the formation of nanoparticles with tailored properties [61]. This method enables precise control over nanoparticle growth and assembly, making it versatile for producing customized nanoparticles and nanocomposites. Careful selection of solvents is essential as it influences precursor solubility, stability of reaction intermediates, and compatibility with desired conditions. Through meticulous solvent selection and parameter optimization, researchers can finely tune the composition, structure, and functionality of synthesized materials [62].

For instance, Shi et al. reported a solvothermal method to prepare TiO_2 and TiO_2/$MoSe_2$ composite

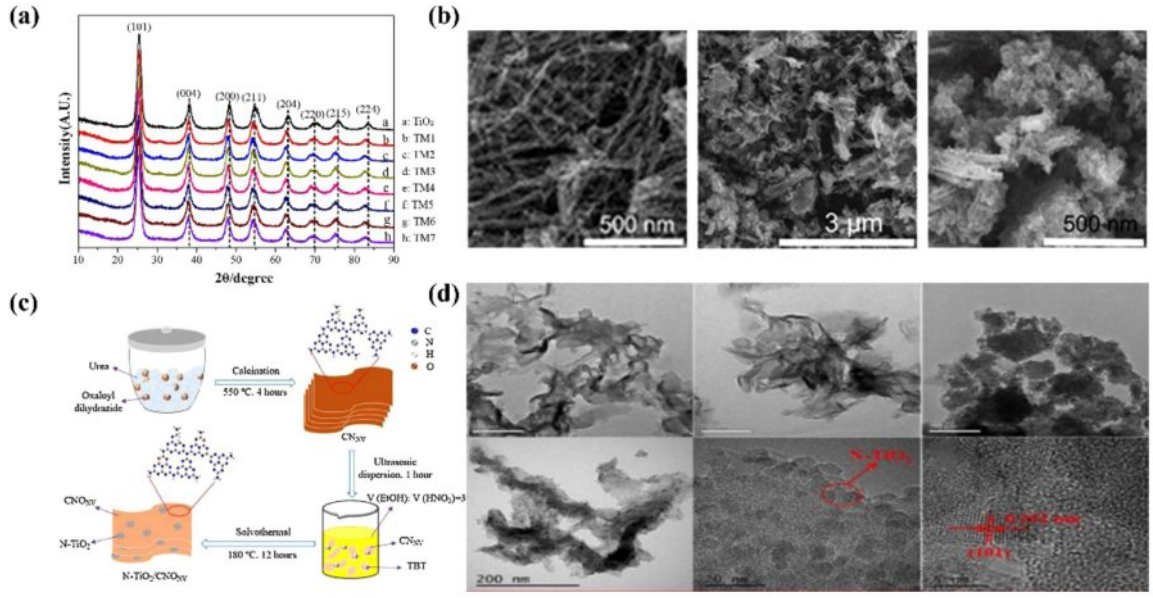

Fig. 5. XRD patterns of the composite photocatalysts with$TiO_2/MoSe_2$ composite loadings (a), FE-SEM images of the corresponding TiO_2 powders (b), formation pathway and TEM images of hollow N-TiO_2/CNO_{NV} heterojunction photocatalyst (c) and (d).

photocatalysts for evaluating the catalytic activity of TiO_2 [63]. The XRD patterns of TiO_2 and $TiO_2/MoSe_2$ composite structures is displayed in Fig. 5a. Chu et al. employed a solvothermal method to modify mesoporous anatase titanium dioxide nanomaterials (MATNs), achieving a desired transformation in their structure in Fig. 6b [64]. Similarly, Wang et al. synthesized N-TiO_2/O doped N vacancy g-C_3N_4 using solvothermal techniques, enhancing the properties of TiO_2/g-C_3N_4 composites [65]. The formation pathway and TEM images of hollow N-TiO_2/CNO_{NV} heterojunction photocatalyst are shown in Fig. 6c and d, respectively. Lv et al. prepared GO/TiO_2/Bi_2WO_6 (GTB) nanocomposites via solvothermal synthesis, combining the advantageous properties of graphene, TiO_2, and Bi_2WO_6 [66].

In conclusion, solvothermal methods offer effective means for tailoring the properties of advanced photocatalytic materials, and solvothermal synthesis allowing precise control over material properties using organic solvents with higher boiling points.

Template methodology

The template method is an effective approach for synthesizing TiO_2-based nanomaterials with precise structures and controlled morphology [49]. It employs templates that can be removed either physically or chemically, resulting in nanomaterials with consistent sizes, shapes, and distinct properties. Two main types of templates are utilized: soft and hard templates. Soft templates involve the self-assembly of amphiphilic surfactant molecules with titanium dioxide precursors, while hard templates rely on covalent bonds to maintain their structure. These templates are essential for directing the growth and alignment of titanium dioxide nanomaterials [67].

Recent research has delved into various template materials for synthesizing TiO_2. For instance, Zhang et al. utilized polymer-derived mesoporous carbon (PDMC) as a template to synthesize vacancy-rich TiO_{2-x}. The mesopores of PDMC effectively constrained the transition growth of TiO_2, as demonstrated in Fig. 7a [68]. Similarly, Nguyen et al. employed chiral mesoporous gelatin-functionalized cellulose nanocrystals as templates to fabricate mesoporous TiO_{2-x}. Subsequent calcination and ascorbic acid treatment led to the formation of black TiO_{2-x}, depicted in Fig. 7b [69]. Biopolymers indeed offer a promising avenue for transferring template morphology into TiO_2 layers. However, their low thermal stability presents a hurdle in controlling the crystallinity of TiO_2. To tackle this challenge, Chen et al. proposed a novel approach: the cellulose nanofiber (CNF)-guided assembly of TiO_2/CNF films. Through a combination of atomic layer deposition and thermal annealing, they successfully produced polycrystalline TiO_2/CNF films with well-defined morphology. Thermal annealing played a crucial role in shaping the morphology and crystalline state of both TiO_2 and CNF. It notably bolstered the template effect of CNF, as illustrated in Fig. 7c, while also resulting in a higher root-mean-square roughness due to the collapse of voids in the 3D CNF network [70]. Additionally, the partially carbonized cellulose bundles within the remaining CNF network contributed to the electron density of the polycrystalline TiO_2 nanoparticles. This innovative strategy not only addresses the issue of biopolymer thermal stability but also opens up new possibilities for controlled synthesis of TiO_2 films with desired properties.

Furthermore, Zhang et al. introduced a biological

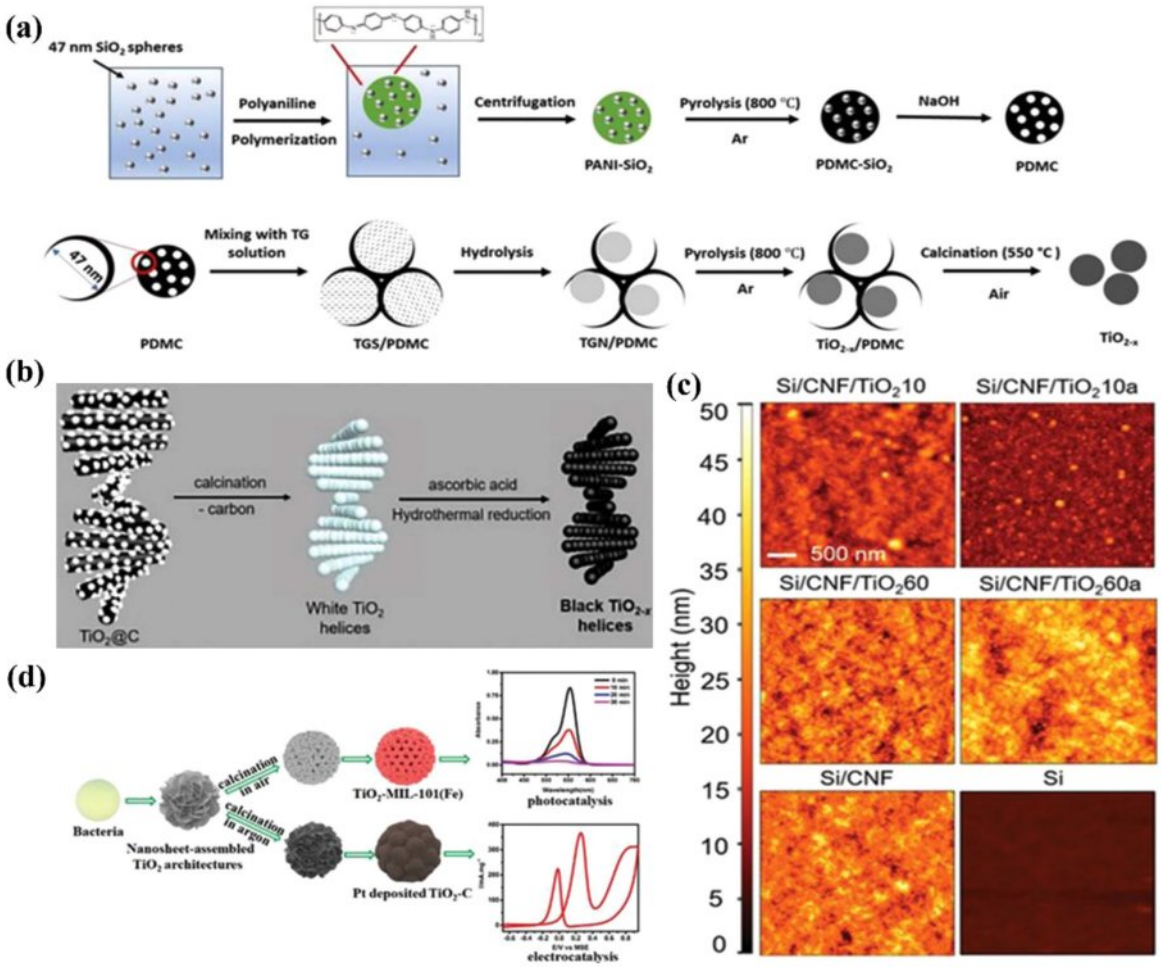

Fig. 6. (a) TiO_{2-x}/PDMC and TiO_{2-x} were synthesised by using polymer-derived mesoporous carbontemplates (PDMC) (b)Process for the preparation of chiral nematic mesoporous blackTiO_{2-x} (c) AFM images of TiO_2/CNF (cellulose nanofibril) films on Si substrates (d) synthesis of TiO_2 hierarchical structures for nanosheet assembly and related composites for photocatalysis and electrocatalysis using bacteria as template and reactor.

approach for synthesizing TiO_2 nanosheets, leveraging bacteria as both templates and reactors, and organized them into multistage hierarchical architectures. They achieved control over nanosheet size by regulating the addition of tetrabutyl titanate and H_2O precursors. As depicted in Fig. 7d, diverse compositions and morphologies emerged through calcination under varied atmospheres [71]. One structure resembled nanoporous TiO_2 hollow spheres, while another showcased nanosheet-assembled TiO_2-C hollow spheres. This innovative method not only underscores the versatility of biological templates but also offers a pathway to engineer complex hierarchical TiO_2 structures with tailored properties.

Photocatalyst and Photoelectrochemical Modification Techniques to Enhance H_2 Production of TiO_2

The photocatalyst and photoelectrochemical reaction process involves several stages occurring simultaneously. To fundamentally enhance the catalytic efficiency of semiconductor catalysts, it is crucial to optimize the catalytic efficiency of each photocatalyst and photoelectrochemical reaction process. The goal is to yield highly efficient semiconductor photocatalysts, which is what researchers continually aim for. Concerning the above-mentioned reaction processes, surface modification stands out as the most researched and effective method to improve photocatalyst and photoelectrochemical activity at present [72]. However, for a single semiconductor photocatalyst, it is quite challenging to satisfy the excellent characteristics necessary for the aforementioned reaction processes to proceed smoothly. It can be concluded that strategies for modifying semiconductor surfaces can enhance each stage by designing composite semiconductor catalysts with multiple effects. These multi-effect composite semiconductor catalysts generally include substrate materials, active components, and co-catalysts, which, serve different roles in the reactions according to their naming [73].

TiO_2 metal ion doping

The development of composite semiconductor catalysts has also evolved through various stages. Initially, the research focused primarily on catalysis with a single function, which can be explained from the following perspectives. Metal doping works by introducing metal ions into the material, altering the structure and properties of the material. Doped ions can replace atoms in the material or occupy vacancies, forming new chemical bonds or changing the nature of existing bonds, thus altering the material's conductivity, magnetism, optical properties, and mechanical performance [74-76]. By doping with metal ions, semiconductor materials can be transformed into conductive materials, thereby increasing electrical conductivity [77]. Metal ion doping is one of the effective methods for modifying semiconductors [78].

Moridon [79] reported several methods have been reported to overcome these issues, one of which involves metal ion in TiO_2. The added material can inject electrons directly into the conduction band of TiO_2 and provide a layered bandgap structure, reducing recombination of photo-generated electrons and holes. F. Rodríguez-Hernández [80] examined the impact of transition metal (TM) doping on TiO_2 surfaces for TiO_2-based electrodes used in water splitting electrochemical reactions in Fig. 7a. Two cluster models of TM-doped active sites similar to the anatase TiO_2 (001) and rutile (110) surfaces were considered to evaluate the water splitting reaction when Ti is replaced by TM atoms. These models employed similar representations to address water splitting reactions on pure TiO_2-based electrodes. Cluster structures were viewed as a simplified representation of active sites on the anode of an electrochemical cell, and density functional theory (DFT) was employed to study the oxygen evolution reaction (OER). Simulations were conducted for a group of TMs ranging from vanadium to nickel. The proposed reaction pathways were evaluated by changes in the free energy curves against the externally applied bias. Photocatalysts can be used for air purification and to collect solar energy through water splitting. However, pure TiO_2 photocatalysts are usually inefficient, necessitating the use of co-catalysts to enhance yields. To achieve this, Nejc Rozman [81] prepared TiO_2 and deposited Pt, Ir, and Ru co-catalysts on its surface in Fig. 7b and c. Utilizing two types of basic TiO_2 nanoparticles: P25 and rutile TiO_2 synthesized via hydrothermal methods. Co-catalysts were deposited by wet impregnation using either single elements or combinations of two elements (Pt and Ir, or Pt and Ru), followed by annealing in air or H_2/Ar atmospheres. Annealing in a reducing atmosphere, as opposed to air, enhanced the photocatalytic activity for isopropanol oxidation. They demonstrated a significant effect of co-catalysts on the photocatalytic degradation of isopropanol and the electrochemical water splitting reaction as shown in Fig. 7d. There have been numerous studies on TiO_2 with noble metal co-catalysts. Fuentes et al. [82] investigated the activity of Pt-Ru, Pt-Ir, Pt-Ru-Ir, and Ir-Ru nanoparticle combinations deposited on anatase and rutile TiO_2 in the oxygen evolution reaction (OER). Tanaka [83] prepared TiO_2 deposited with small Pt nanoparticles and larger Au nanoparticles and tested for H_2 yield in Fig. 7e and f. Rutkowska [84] deposited Pt-Ru nanoparticles on multi-walled carbon nanotubes supported TiO_2 for ethanol oxidation.

TiO_2 non-metallic ion doping

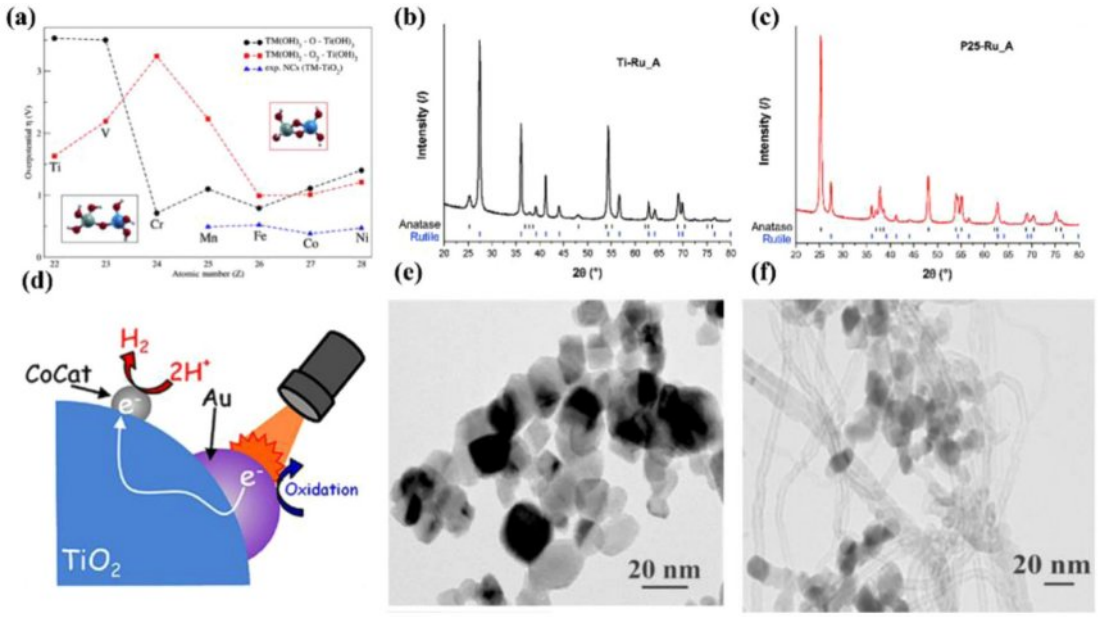

Fig. 7. Reaction of metal doping in TiO_2 (a), xrd spectra of Ru (b) and P25-Ru (c) of doping TiO_2, the mechanism of Au in TiO_2 for water splitting (d), the SEM of Pt (e) and Au (f) doping in TiO_2.

Non-metallic elements doping also can regulate the semiconductor's band structure. Doping ions can form intermediate energy levels within the semiconductor bands, facilitating stepped electron transitions, thus broadening TiO_2's range of light absorption and promoting separation of photoinduced carriers [85]. Although metal ion doping can induce visible light response, the impurity energy levels formed by metal ion doping are typically discontinuous, which is detrimental to hole transfer. Furthermore, the catalytic activity of the catalyst is directly related to the amount of metal ion doping. Excessive doping may turn doping ions into recombination centers for electrons and holes, thereby reducing the photocatalytic activity of the catalyst. In TiO_2 doped with non-metal elements (N, S, C etc.), the p orbitals of the non-metal elements can hybridize with TiO_2's O 2p orbitals, thereby raising the position of TiO_2's valence band and reducing its bandgap energy. Also, non-metal element doping introduces fewer electron-hole recombination sites, hence attracting widespread attention.

It has been reported that C can minimize the bandgap of TiO_2 by producing a hybrid orbital over the valence level of TiO_2 and thus increase visible light absorption. Wang [84] discovered an in-situ growth strategy for synthesizing a 2-D C/TiO_2 heterogeneous hybrid in Fig. 8a. The Ti-C bond as reactive sites, such as platinum behavior, makes it an interesting potential substitute for noble metals in hydrogen evolution. In the absence of noble metals, the C/TiO_2 hybrid exhibits a significant enhancement of hydrogen evolution from water splitting using solar light ~3.046 mmol h^{-1} g^{-1}. Zhou [86] prepared C-TiO_2 thin film on ITO substrate by pulsed laser deposition, which found that the C doping in TiO_2 narrowed the band gap of the C-TiO_2 from 3.25 eV of pure TiO_2 to 3.15 eV in Fig. 8b. The photoelectrochemical property of the C-TiO_2 film was examined by evaluating the efficiency of hydrogen generation by water splitting in a two-compartment electrochemical system. Wang [87] prepared S doping in TiO_2 via low-temperature hydrothermal oxidation and found it can effectively narrow the bandgap of TiO_2 due to the fact that S 3p level is higher than O 2p orbital as shown in Fig. 8c. In addition, the N doping in TiO_2 is another way to enhance the performance of photocatalytic water splitting for hydrogen. Kumar [88] reported a facile one-step synthesis of N-doped TiO_2 nanotubes using nitrogen gas as a nitrogen source in Fig. 8d. N-doped TiO_2 exhibits enhanced visible-light photocatalytic activity toward the photoelectrochemical water-splitting reaction and high stability due to nitrogen doping and band-gap narrowing. N-doped TiO_2 exhibit unique and efficient photoelectrochemical cell (PEC) water-splitting activity for H_2 generation in aqueous electrolytes with a pH gradient. Wang [89] doped N in TiO_2 for boosting the visible light absorption properties. The experimental results show that the crystal structure is anatase phase, and the concentration of substitutional nitrogen is 4.91 % which leads to a narrow optical band gap of 2.65 eV. Lee [90] observed that the nitrogen-doped film electrode's photoelectrochemical response significantly improves as compared to undoped TiO_2 as exposed to light.

Heterojunction of TiO_2

Compounding two semiconductors with suitable

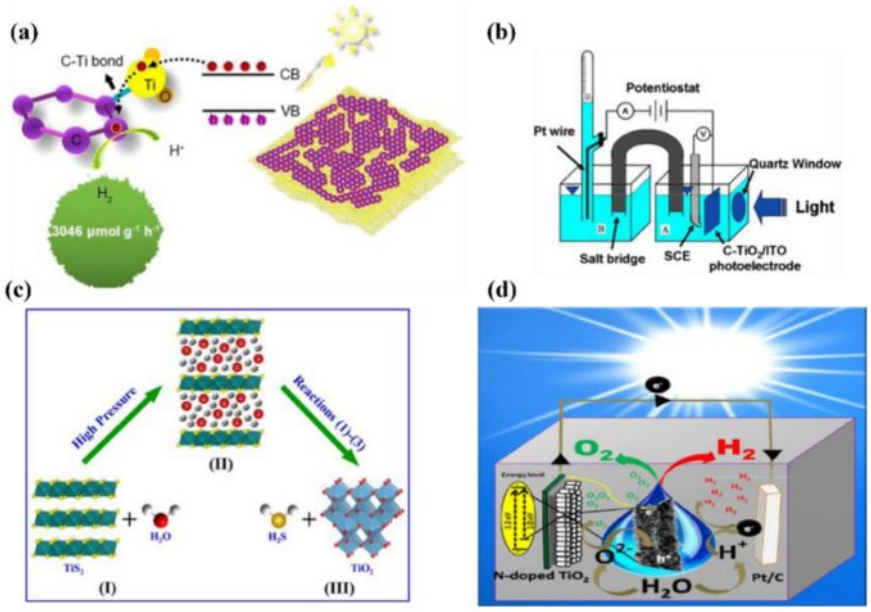

Fig. 8. the performance of C-TiO_2 in hydrogen evolution (a), schematic diagram of the two-chamber C-TiO_2 PEC system (b), chemical reaction process for the hydrothermal oxidation of S-TiO_2 (c), N-doped TiO_2 nanotubes as a photoanode used in PEC water-splitting application for hydrogen generation (d).

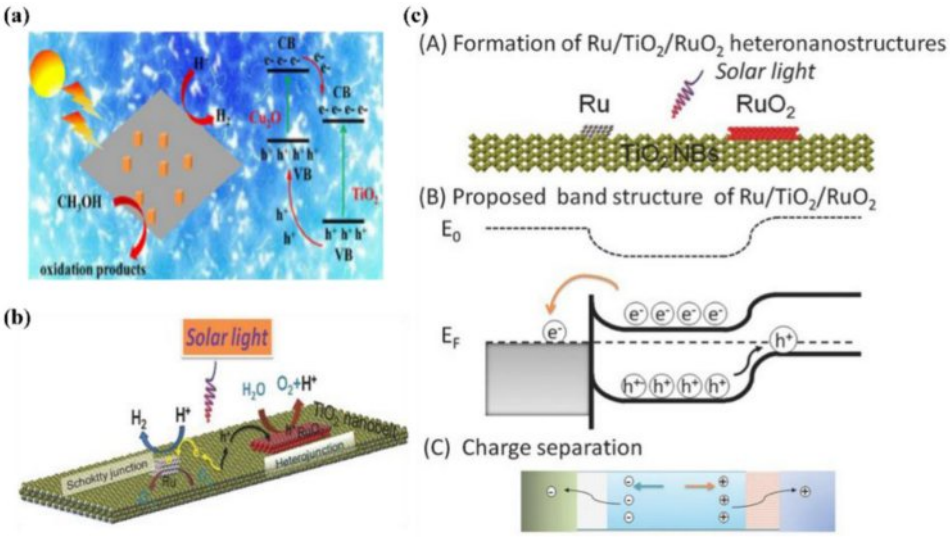

Fig. 9. the schematic diagram of Cu_2O/TiO_2 heterostructure for H_2 evolution (a), Proposed mechanism for the photocatalytic water splitting into H_2 over the Ru-modified TiO_2 NBs under solar light irradiation (b) and schematic illustration of the proposed band structure of the $Ru/TiO_2/RuO_2$ in the junctions (c).

bandgap positions and utilizing the difference in their energy band structures to form a potential difference, thereby changing the migration path of photogenerated electron holes, can effectively promote the separation efficiency of photogenerated carriers. Chen [91] constructed a Cu_2O/TiO_2 heterostructure material, and with a load mass ratio of 6%, its photocatalytic activity for hydrogen production by water splitting was 416 times that of Cu_2O and 49 times that of TiO_2. This is attributed to the heterojunction built between the two with suitable bandgaps in Fig. 9a. To verify the mechanism of study, the conduction band of Cu_2O is at -0.89 eV, and the valence band position of TiO_2 is at 2.76 eV, with Cu_2O being a p-type semiconductor and TiO_2 a n-type semiconductor. When the interfaces of the two come into contact, an internal electric field is formed. Under the effect of this internal electric field, electrons and holes migrate according to the Type-II alignment mechanism. Gu [92] reported a photocatalyst based on a post-thermal oxidation wet impregnation reduction method to modify TiO_2 nanobelts (NBs) with metal Ru and RuO_2 dual cocatalysts. Detailed characterization of the samples was carried out, and their photocatalytic activity for semi-splitting and total splitting reactions under sunlight was systematically evaluated. The detailed characterization and analysis clearly revealed the formation of a Schottky junction at the Ru-TiO_2 interface and a RuO_2/TiO_2 hetero-junction. The photocatalyst test results show that both Ru and RuO_2 enhance the photocatalytic H_2/O_2 evolution and water-splitting activity. Furthermore, co-modification with dual cocatalysts Ru and RuO_2 can further enhance the photocatalytic activity of TiO_2 NBs. The RuO_2/TiO_2 heterojunction improves the transfer of photogenerated holes from TiO_2 to RuO_2, with water undergoing hole oxidation to evolve O_2, while the Ru/TiO_2 heterojunction improves the transfer of photogenerated holes in Fig. 9b and c.

Yan [93] have studied semiconductor-based Z-scheme overall water splitting extensively for the production of hydrogen fuel from renewable resources in Fig. 10a. The Z-scheme involves two different types of semiconductors photocatalysts as well as closely related oxidation-reduction processes. However, the two separate photocatalytic processes necessitate good carrier generation and separation, which greatly limits the efficiency of overall water splitting. Here, to address the issue of photogenerated carrier recombination, Yan's team has developed a one-step hydrothermal method to synthesize a TiO_2/C_3N_4 hetero-junction. Layered g-C_3N_4 provides a template and guidance for the heteronucleation of anatase TiO_2 with exposed (001) facets. As TiO_2 grows, bulk g-C_3N_4 self-exfoliates into thicker nanosheets. The heterojunction with exposed TiO_2 (001) facets ensures the effective separation of photogenerated carriers, thus enhancing photocatalytic hydrogen evolution in Fig. 10b. Wei [94] prepared a hydrogenated TiO_2 anatase/rutile phase heterojunction and used it for photoelectrochemical water splitting to produce clean H_2 energy under sunlight. This TiO_2 phase heterostructure photocatalyst material with a core-shell structure was precisely fabricated by hydrothermal growth of rutile TiO_2 nanorod arrays as a core and subsequent formation of a thickness-controlled anatase TiO_2 layer as a shell using ALD technology, followed by hydrogenation. Introduction of some disorder structures and oxygen vacancies to the TiO_2 phase heterostructure. This novel TiO_2 photocatalyst material exhibited a photocurrent of 3.88 mA cm^{-1} The high photocurrent density is amplified by 2 spaces at the beginning of the paragraph, reaching a maximum

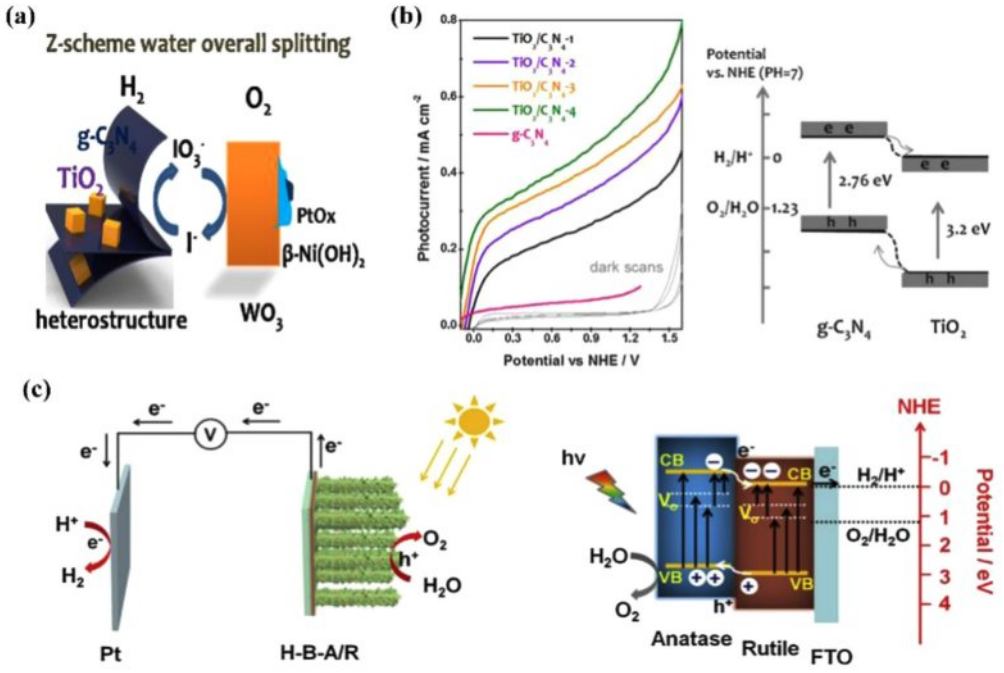

Fig. 10. the schematic illustration of heterojunction formed between g-C_3N_4 and TiO_2 (a), Photocurrent response of samples in 0.5 M Na_2SO_4 solution with the scan rate of 50 mVs^{-1} from negative to positive potential (b), schematic for the proposed mechanism of PEC water splitting and the energy band structure of the hydrogenated anatase/rutile branched TiO_2 NRs (c).

IPCE of 59.7% at a wavelength of 380 nm. These figures are almost 3.8 times and 7.4 times higher compared to the bare rutile TiO_2, respectively. The enhancement in photoelectrochemical performance is primarily attributed to the synergistic effect of the hot electron core-shell heterostructures as shown in Fig. 10c.

Conclusion

This paper focuses on the research progress of photocatalytic hydrogen production using TiO_2 catalyst and its influencing factors. The energy problems caused by the global shortage of fossil energy and the environmental problems caused by the burning of large amounts of fossil energy cannot be underestimated. H_2 energy is an ideal clean energy source, the main source of hydrogen energy is water, and what is produced by the burning of hydrogen is also water (non-toxic and non-polluting). It has high exothermic value, which makes it the most ideal substitute for traditional energy. Solar photocatalytic decomposition of water to produce hydrogen is the conversion of solar energy into chemical energy (hydrogen energy) conversion process, as a new type of hydrogen production technology, but also one of the best means to solve energy and environmental problems. Therefore, exploring the development of photocatalytic hydrogen-producing materials with low cost and high efficiency of hydrogen production is an ongoing concern for researchers. TiO_2 is considered to be the optimal photocatalytic material nowadays due to its high chemical and thermal stability, as well as the fact that it is not easy to be photocorroded or chemically corroded during the reaction, and it is non-polluting, cheap and easy to be obtained.

However, as a common photocatalyst, TiO_2 cannot be easily applied in photocatalysis due to its wide bandgap energy that can only be activated under ultraviolet light. Before migrating to the surface to decompose water, it occupies 2%-5% of the solar spectrum and the higher complex rate of photogenerated charge carriers, which limits its photocatalytic performance. This greatly restricts the practical application of TiO_2 as a photocatalytic material. In addition, TiO_2 also exists the influence of its own crystalline phase. The higher forbidden band width of anatase makes its electron-hole pairs have more positive or more negative potentials. Thus, it has a higher oxidation ability. The surface adsorption of anatase has a stronger ability to adsorb H_2O, O_2 and OH^-, resulting in higher photocatalytic activity for hydrogen evolution. During the crystallization process, anatase grains usually have smaller size and larger specific surface area, which is favorable for photocatalytic reaction. To improve the photocatalytic efficiency of photocatalytic materials has been a major problem in the current research, we can broaden the wavelength of TiO_2 absorption by doping metal ions metal ions can be introduced in the TiO_2 forbidden band than the TiO_2 conduction band of the impurity energy level is lower than the TiO_2 conduction band. The TiO_2 absorbs a wider range of wavelengths of the visible light, so that the valence band excitation

of electrons transferred to the impurity level. Then it continues to absorb the energy, and electrons by the impurity level leap to the conduction band. at the same time, the valence band excited electron transfer to the impurity level. Leap to the conduction band, while inhibiting the compounding of electrons and holes can be introduced in the TiO_2 lattice defects, the formation of shallow potential capture traps captures electrons and holes, prolonging the time of the compounding of electrons and holes, thereby inhibiting the compounding of electrons and holes in order to increase the forbidden band width. Or non-metal ion doping embeds in the TiO_2 lattice to reduce the forbidden bandwidth and make TiO_2 with visible light response. It can effectively increase the sensitivity of TiO_2 and thus significantly enhance the photocatalytic ability so as to improve the photocatalytic activity. Semiconductor heterojunction can also be used, in which when light irradiates the surface of TiO_2 heterojunction, photons are absorbed and electrons in the material are excited, generating photogenerated electrons and holes. Among them, the photogenerated electrons have high reducing ability and can participate in the oxidation reaction; the holes have strong oxidizing ability and can participate in the reduction reaction. Therefore, the separation of photogenerated electrons and holes is the key to realize efficient photocatalysis. Meanwhile, the research of related scholars mainly focuses on the modification of TiO_2 to reduce the compound rate of electron-hole pairs to improve the utilization rate of visible light, so as to increase the photocatalytic efficiency of TiO_2, which can increase the efficiency of hydrogen production at the source.

However, there are still many problems to be solved around the TiO_2, such as the wavelength of visible light is 400~800 nm and system of electrons and holes in the rapid composite (composite time of nanoseconds). Hence, future research efforts need to continue to improve the light absorption capacity and to find new ways to let the electrons and holes in the rapid separation of TiO_2. The conduction band potential of TiO_2 is 2.92 eV, and the generated holes have strong oxidizing ability, which can oxidize most of the organic matter, so we should continue to improve the separation rate of electrons and holes. It is a good way to make full use of the oxidizing ability of the TiO_2 holes. The introduction of other substances into TiO_2, on the one hand, will lead to complexity of the preparation method and the cost of the enhancement. On the other hand, the substances used for modification may also pollute the environment, such as adding heavy metal ions and harmful organic substances to modify TiO_2. Photocatalytic technology is one of the green and efficient strategies to deal with the current energy shortage and environmental pollution, and the development of stable and efficient photocatalysts has always been the goal of researchers, and TiO_2 as an important photocatalytic material has a wide range of prospects for application and research value. As one of the most commonly used and optimal photocatalytic materials, it is of great importance to investigate and improve the photocatalytic efficiency of TiO_2. At present, only solar cells have been popularized in the application of titanium dioxide photocatalysis, but with the progress of science and technology and the continuous innovation and development of photocatalysis, the semiconductor photocatalytic reaction of hydrogen technology is developing rapidly, and it is expected to become an important method of mass hydrogen production in the future.

References

1. X. Zhang and S.P. Jiang, Mater. Today Energy 23 (2022) 100904.
2. M.G. Lee, J.W. Yang, H. Park, C.W. Moon, D.M. Andoshe, J. Park, C.-K. Moon, T.H. Lee, K.S. Choi, and W.S. Cheon, Nano-Micro Lett. 14[1] (2022) 48.
3. Y.-n. Jiang, M. Zhang, X. Zhang, and Y. Ma, J. Phys. Chem. C 126[8] (2022) 3915-3922.
4. X. Zhang, S. Zhang, X. Cui, W. Zhou, W. Cao, D. Cheng, and Y. Sun, Chem-Asian J. 17[20] (2022) e202200668.
5. T.L. Nguyen, T.H. Pham, Y. Myung, S.H. Jung, M.H. Tran, M.G. Mapari, Q. Van Le, M.V. Nguyen, T.T.H. Chu, and T. Kim, Int. J. Hydrogen Energy 47[98] (2022) 41621-41630.
6. M. Han, Z. Wang, Z. Zhang, S. Wang, G. Wang, K. Hou, H. Zhang, L. Jiang, and G. Hu, Chem. Eng. Sci. 281 (2023) 119-151.
7. W. Liu, L. Sun, Z. Li, M. Fujii, Y. Geng, L. Dong, and T. Fujita, Environ. Sci. Pollut. Res. Int. 27[25] (2020) 31092-31104.
8. J.D. Holladay, J. Hu, D.L. King, and Y. Wang, Catal. Today 139[4] (2009) 244-260.
9. T.L. Levalley, A.R. Richard, and M. Fan, Int. J. Hydrogen Energy 39[30] (2014) 16983-17000.
10. K.M. Rena, B. Zacharia, S. Machhirake, N.P. Kim, S.-H. Lee, B.-D. Jeong, H. Singh, L. Kumar, S. Kumar, Rakesh, Bioresour. Technol. 309[1] (2020) 123297.
11. F.E. Chakik, M. Kaddami, and M. Mikou, Int. J. Hydrogen Energy 42[40] (2017) 25550-25557.
12. S. Shiva Kumar, and V. Himabindu, Mater. Sci. Energy Technol. 2[3] (2019) 442-454.
13. K.G. dos Santos, C.T. Eckert, E. De Rossi, R.A. Bariccatti, E.P. Frigo, C.A. Lindino, and H.J. Alves, Renew. Sust. Energ. Rev. 68 (2017) 563-571.
14. S. Wang, A. Lu, and C. Zhong, Nano. Converg. 8[01] (2021) 1-23.
15. A. Fujishima and K. Honda, Nature 238[5358] (1972) 37-38.
16. K.H. Ng, S.Y. Lai, C.K. Cheng, Y.W. Cheng, and C.C. Chong, Chem. Eng. J. 417 (2021) 128847.
17. Y.H. Hong, Y. Lee, W. Nam, and S. Fukuzumi, J. Am. Chem. Soc. 144[02] (2022) 695-700.
18. R. Huang and X. Yang, J. Ceram. Process. Res. 23[02] (2022) 213-220.
19. Z. Cheng, Z. Hu, X. Ma, M. Wang, N. Gan, and M. Pan, J. Phys. Chem. C 126[28] (2022) 11510-11517.
20. Y. Lin, W. Fang, R. Xv, and L. Fu, Int. J. Hydrogen Energy 47[78] (2022) 33361-33373.
21. A. Mishra, A. Mehta, S. Basu, N.P. Shetti, K.R. Reddy, and T.M. Aminabhavi, Carbon 149 (2019) 693-721.

22. F. Song, Y. Sun, and P. Rao, J. Ceram. Process. Res. 22[05] (2021) 521-526.
23. Z. Kang, H. Si, S. Zhang, J. Wu, Y. Sun, Q. Liao, Z. Zhang, and Y. Zhang, Adv. Funct. Mater. 29[15] (2019).
24. C.M. Wolff, P.D. Frischmann, M. Schulze, B.J. Bohn, R. Wein, P. Livadas, M.T. Carlson, F. Jaeckel, J. Feldmann, F. Wuerthner, and J.K. Stolarczyk, Nat. Energy 3[10] (2018) 862-869.
25. M.-Y. Xie, K.-Y. Peng, X.-Y. Wu, R.-J. Chavali, M. Chang, and W. Chen, J. Taiwan Inst. Chem. Eng. 70 (2017) 161-167.
26. G. Wang, C. Zhang, W. Zhao, B. Wang, Y. Liu, T. Zhang, W. Cui, R. Zhang, and Z. Zhao, Ccs. Chem. 6[06] (2024) 1523-1534.
27. X.P. Feng, L. Sun, W. Wang, Y. Zhao, and J. Shi, Sep. Purif. Technol. 324 (2023) 124520.
28. M. Ismael, Sol. Energy 211 (2020) 522-546.
29. A. Maddu, I. Deni, and I. Sofian, J. Ceram. Process. Res. 19[01] (2018) 25-31.
30. S. Kim, Y. Cho, R. Rhee, and J.H. Park, Carbon Energy 2[01] (2020) 44-53.
31. R. Dholam, N. Patel, M. Adami, and A. Miotello, Int. J. Hydrogen Energy 34[13] (2009) 5337-5346.
32. S. Lin, H. Ren, Z. Wu, L. Sun, X.G. Zhang, Y.M. Lin, K. H.L. Zhang, C.J. Lin, Z.Q. Tian, and J.F. Li, J. Energy Chem. 59 (2021) 721-729.
33. A. Tanaka, K. Teramura, S. Hosokawa, H. Kominami, and T. Tanaka, Chem. Sci. 8[4] (2017) 2574-2580.
34. Z. Chen, X. Liang, X. Fan, J. Wang, A. Huang, and Z. Liu, Chin. J. Mater. Res. 33[7] (2019) 515-522.
35. R.B. Ali, Q.A. Sial, Y.J. Lee, M. Waqas, S.S. Kalanur, and H. Seo, J. Asian Ceram. Soc. 11[3] (2023) 424-435.
36. L.R. Sheppard, S. Hager, J. Holik, R. Liu, S. Macartney, and R. Wuhrer, J. Phys. Chem. C 119[1] (2015) 392-400.
37. D. Kim, S. Kang, and K. Kim, J. Ceram. Process. Res. 24[5] (2023) 807-815.
38. S. Termnak, W. Triampo, and D. Triampo, J. Ceram. Process. Res. 10[04] (2009) 491-496.
39. H. Sutrisno and Sunarto, J. Ceram. Process. Res. 18[05] (2017) 378-384.
40. P.H. Borse, C.R. Cho, K.T. Lim, T.E. Hong, E.D. Jeong, J.H. Yoon, S.M. Yu, and H.G. Kim, J. Ceram. Process. Res. 13[01] (2012) 42-46.
41. Y. Kang, K. Song, J. Park, Y.C. Kim, and S. Oh, J. Ceram. Process. Res. 14[03] (2013) 419-425.
42. S. Narakaew, J. Ceram. Process. Res. 18[01] (2017) 36-40.
43. Y. Song, S. Son, D.Y. Lee, M. Lee, and B. Kim, J. Ceram. Process. Res. 17[11] (2016) 1197-1201.
44. V. Kumaravel, S. Mathew, J. Bartlett, and S.C. Pillai, Appl. Catal. B-Environ. 244 (2019) 1021-1064.
45. K. Park, Y.J. Kim, T. Yoon, S. David, and Y.M. Song, Rsc Adv. 9[52] (2019) 30112-30124.
46. M. Sawal, A. Jalil, N. Khusnun, N. Hassan, and M. Bahari, Electrochim. Acta 467 (2023) 143142.
47. C. Chen, B. Yu, P. Liu, J. Liu, and L. Wang, J. Ceram. Process. Res. 12[04] (2011) 420-425.
48. M.R. Vaezi and A.E. Kandjani, J. Ceram. Process. Res. 15[06] (2014) 376-381.
49. A. Yazdani, H.R. Rezaie, and H. Ghassai, J. Ceram. Process. Res. 11[03] (2010) 348-353.
50. X. Lin, M. Sun, B. Gao, W. Ding, Z. Zhang, S. Anandan, and A. Umar, J. Alloys Compd. 850 (2021) 156653.
51. S. Chuangchote, J. Jitputti, T. Sagawa, and S. Yoshikawa, ACS Appl. Mater. Interfaces 1[5] (2009) 1140-1143.
52. X. Li, W. Zheng, G. He, R. Zhao, and D. Liu, Acs. Sustain. Chem. Eng. 2[2] (2014) 288-295.
53. X. Zhang, Y. Sun, X. Cui, and Z. Jiang, Int. J. Hydrogen Energy 37[1] (2012) 811-815.
54. Z. Meng, L. Zhu, C.S. Lim, K. Ullah, S. Ye, K. Cho, and W. Oh, J. Ceram. Process. Res. 14[03] (2013) 349-354.
55. H. Guo, N. Jiang, H. Wang, K. Shang, N. Lu, J. Li, and Y. Wu, Appl. Catal. B-Environ. 248 (2019) 552-566.
56. A. Crake, K.C. Christoforidis, A. Gregg, B. Moss, A. Kafizas, and C. Petit, Small 15[11] (2019) 1805473.
57. B. Jiang, C. Tian, W. Zhou, J. Wang, Y. Xie, Q. Pan, Z. Ren, Y. Dong, D. Fu, and J. Han, Chem. Eur. J. 17[30] (2011) 8379-8387.
58. S. Kaowphong, T. Thongtem, and S. Thongtem, J. Ceram. Process. Res. 11[4] (2010) 432-436.
59. M. Najafi, M. Vaezi, and S. Sadrnezhaad, J. Ceram. Process. Res. 12[6] (2011) 695-698.
60. S. Kaowphong, T. Thongtem, and S. Thongtem, J. Ceram. Process. Res. 11[04] (2010) 432-436.
61. M. Najafi, M.R. Vaezi, and S.K. Sadrnezhaad, J. Ceram. Process. Res. 12[06] (2011) 695-698.
62. X. Wang, J. Zhuang, Q. Peng, and Y. Li, Nature 437[7055] (2005) 121-124.
63. F. Shi, C. Xing, and X. Wang, Int. J. Hydrogen Energy 46[78] (2021) 38636-38644.
64. L. Chu, J. Zhang, W. Liu, R. Zhang, J. Yang, R. Hu, X. a. Li, and W. Huang, Acs. Sustain. Chem. Eng. 6[4] (2018) 5588-5597.
65. Y. Wang, L. Rao, P. Wang, Z. Shi, and L. Zhang, Appl. Catal. B-Environ. 262 (2020) 118308.
66. N. Lv, Y. Li, Z. Huang, T. Li, S. Ye, D.D. Dionysiou, and X. Song, Appl. Catal. B-Environ. 246 (2019) 303-311.
67. W. Lee and S.-J. Park, Chem. Rev. 114[15] (2014) 7487-7556.
68. T. Zhang, J. Low, J. Yu, A.M. Tyryshkin, E. Mikmeková, and T. Asefa, Angew. Chem. Int. Edit. 59[35] (2020) 15000-15007.
69. T.D. Nguyen, J. Li, E. Lizundia, M. Niederberger, W.Y. Hamad, and M.J. MacLachlan, Adv. Funct. Mater. 29[40] (2019) 1904639.
70. Q. Chen, M. Betker, C. Harder, C.J. Brett, M. Schwartzkopf, N.M. Ulrich, M.E. Toimil-Molares, C. Trautmann, L.D. Söderberg, and C.L. Weindl, Adv. Funct. Mater. 32[6] (2022) 2108556.
71. S. Zhang, H. Li, S. Wang, Y. Liu, H. Chen, and Z.-X. Lu, ACS Appl. Mater. Interfaces 11[40] (2019) 37004-37012.
72. H. Eidsvåg, S. Bentouba, P. Vajeeston, S. Yohi, and D. Velauthapillai, Molecules 26[6] (2021) 1687.
73. M. Ge, Q. Li, C. Cao, J. Huang, S. Li, S. Zhang, Z. Chen, K. Zhang, S.S. Al-Deyab, and Y. Lai, Adv. Sci. 4[1] (2017) 1600152.
74. H.H. Nguyen, G. Gyawali, and B. Joshi, J. Ceram. Process. Res. 23[01] (2022) 33-40.
75. K.D.T. Kien, N.V.U. Nhi, H.N. Minh, and D.Q. Minh, J. Ceram. Process. Res. 23[3] (2022) 350-355.
76. M. Ji and Y.-I. Lee, J. Ceram. Process. Res. 22[4] (2021) 386-393.
77. Y. Song, M. Lee, B. Kim, and D.Y. Lee, J. Ceram. Process. Res. 20[02] (2019) 182-186.
78. P.S. Basavarajappa, S.B. Patil, N. Ganganagappa, K.R. Reddy, A. V. Raghu, and C.V. Reddy, Int. J. Hydrogen Energy 45[13] (2020) 7764-7778.
79. S.N.F. Moridon, K. Arifin, R.M. Yunus, L.J. Minggu, and M.B. Kassim, Ceram. Int. 48[5] (2022) 5892-5907.
80. F. Rodríguez-Hernández, D. Tranca, A. Martínez-Mesa,

L. Uranga-Piña, and G. Seifert, J. Phys. Chem. C 120[45] (2016) 25851-25860.
81. N. Rozman, P. Nadrah, R. Cornut, B. Jousselme, M. Bele, G. Dražić, M. Gaberšček, Š. Kunej, and A.S. Škapin, Int. J. Hydrogen Energy 46[65] (2021) 32871-32881.
82. R.E. Fuentes, J. Farell, and J.W. Weidner, Electrochem. Solid St. 14[3] (2010) E5.
83. A. Tanaka, S. Sakaguchi, K. Hashimoto, and H. Kominami, Acs. Catal. 3[1] (2013) 79-85.
84. S.L. Wang, J. Li, S. Wang, J.E. Wu, T.I. Wong, M.L. Foo, W. Chen, K. Wu, and G.Q. Xu, Acs. Catal. 7[10] (2017) 6892-6900.
85. M. Grandcolas and J. Ye, J. Ceram. Process. Res. 13[01] (2012) 65-70.
86. B. Zhou, M. Schulz, H. Lin, S.I. Shah, J. Qu, and C. Huang, Appl. Catal. B-Environ. 92[1-2] (2009) 41-49.
87. F. Wang, F. Li, L. Zhang, H. Zeng, Y. Sun, S. Zhang, and X. Xu, Mater. Res. Bull. 87 (2017) 20-26.
88. M.P. Kumar, R. Jagannathan, and S. Ravichandran, Energ. Fuel. 34[7] (2020) 9030-9036.
89. C. Wang, Q. Hu, J. Huang, L. Wu, Z. Deng, Z. Liu, Y. Liu, and Y. Cao, Appl. Surf. Sci. 283 (2013) 188-192.
90. W.-J. Lee, S.-J. Hong, S.-H. Kim, B.-H. Kim, A. Wakahara, and J.-W. Moon, J. Ceram. Process. Res. 9[1] (2008) 38-41.
91. J.-L. Chen, M.-M. Liu, S.-Y. Xie, L.-J. Yue, F.-L. Gong, K.-M. Chai, and Y.-H. Zhang, J. Mol. Struct. 1247 (2022) 131294.
92. Q. Gu, Z. Gao, S. Yu, and C. Xue, Adv. Mater. Interfaces 3[4] (2016) 1500631.
93. J. Yan, H. Wu, H. Chen, Y. Zhang, F. Zhang, and S.F. Liu, Appl. Catal. B-Environ. 191 (2016) 130-137.
94. N. Wei, Y. Liu, M. Feng, Z. Li, S. Chen, Y. Zheng, and D. Wang, Appl. Catal. B-Environ. 244 (2019) 519-528.